Emergent Materials
https://doi.org/10.1007/s42247-024-00851-6

ORIGINAL ARTICLE

Zein nanoencapsulation enhances the antifungal activity of thymol for postharvest decay control in bananas

Dana C. Punelas–Villanueva[1,2] · Ronaniel A. Almeda[1,3] · Mari Sherlin S. Chua[1] · Rico F. Tabor[4] · Mark Louis P. Vidallon[1,4,5,6,7] · Evelyn B. Rodriguez[1]

Received: 21 June 2024 / Accepted: 22 August 2024

Abstract
The current work describes a nanoparticle system-based approach to enhance the antifungal activity of thymol, a ubiquitous natural antifungal phenolic compound, in postharvest control against banana anthracnose. Thymol was encapsulated within the amphiphilic protein zein by high-shear emulsification, yielding highly dispersible thymol-loaded zein nanoparticles with a high encapsulation efficiency (70%). These particles have an average diameter of 300 nm with spherical morphology, smooth interface, and matrix-type internal structure, as supported by comprehensive structural characterization (dynamic light scattering, transmission electron microscopy and atomic force microscopy). Based on a 40-d storage stability test, thymol was effectively retained within the nanoparticles at 4 °C and ambient room temperature (99% and 97% retention, respectively), despite thymol's instability and volatility. Antifungal activity assessment against *Colletotrichum musae,* one of the predominant pathogens that cause banana anthracnose, showed a 200- to 300-fold improvement in the in vitro antifungal activity of thymol. Moreover, the application of thymol-loaded zein nanoparticles as a spray component for banana postharvest treatment demonstrated the efficacy of thymol-loaded zein nanoparticles in preventing and delaying the formation of initial symptoms of banana anthracnose. This appears to arise from the thymol-loaded zein nanoparticles depositing as a film on the banana epidermis, as revealed by atomic force microscopy. Overall, this nanoparticle system offers a new avenue for the design of effective antifungal materials with potential applications in combatting postharvest diseases.

Keywords Banana anthracnose · Nanoencapsulation · Postharvest control · Thymol · Zein

1 Introduction

Postharvest diseases pose a significant risk to the agricultural industry, leading to crop losses during transportation and contributing to the food waste epidemic that modern society faces. In particular, anthracnose caused by the fungus *Colletotrichum musae* (C. *musae*) is a major postharvest disease affecting banana fruits, which results in 30–40% losses in commercial value. This fungus infects young banana fruit but goes unrecognized until the fruit turns ripe and yellow [1]. Therefore, it is crucial to implement effective measures to mitigate such risks [2].

Various postharvest treatments aim to preserve produce quality and extend shelf life. These methods are broadly categorized into chemical, physical, and gaseous treatments. Chemical treatments involve substances such as hydrogen peroxide, chlorine-based solutions, and fungicides to inhibit microbial growth, prevent browning, and reduce respiration and water loss [3, 4]. Gaseous treatments include ozonation and modified atmosphere packaging, which help maintain cell wall integrity and delay senescence [5]. Physical treatments, like edible coatings and heat applications, also play a role in controlling spoilage. Edible coatings create a moisture and oxygen barrier while heat treatments target spores and microorganisms, and irradiation serves as a quarantine method [6, 7]. Chemical treatments such as application of synthetic fungicides offer cost-effective and efficient solutions to delay senescence, reduce spoilage, and enhance the marketability of crops, making them a popular choice for improving yields and quality [8–10]. However, their use can pose risks to environmental fate, food safety, and human health due to the bioaccumulation of contaminants in food chains, residual effects on soil and food, development of

Dana C. Punelas–Villanueva and Ronaniel A. Almeda are equally contributing first authors.

Extended author information available on the last page of the article

Published online: 16 September 2024

pathogen resistance, and various health disorders. These issues have received considerable critical attention, leading to an increased demand for a new generation of more sustainable and less toxic technological interventions [11, 12].

Bioactive substances from plants, and other natural compounds such as secondary metabolites, active enzymes and volatiles such as essential oils (EOs) are a rich supply of antifungal compounds, making them ideal bactericides and fungicides for the treatment of post-harvest fungal infections [13]. Various research have demonstrated that EO 'biopesticides' with Generally Recognized as Safe (GRAS) status have excellent antibacterial and antifungal performance, particularly in food sanitation and plant pathogen control, and have several advantages including low environmental impact, high biodegradability, reduced toxicity, and cost-effectiveness for farmers. Essential oils such as lemon grass oil, [14] basil essential oil, [15] thymol, [16] carvacrol, [17] cinnamon oil, [18] and oregano oil [19] are some of the most widely studied essential oils for postharvest control of microorganisms.

In particular, thymol (2-isopropyl-5-methylphenol), the main phenolic compound in oregano (*Origanum vulgare*), wild bergamot (*Monarda fistulosa*) and thyme (*Thymus vulgaris*) EOs, has been effective in controlling postharvest diseases in blueberry fruits and tomatoes [20–22]. Also, wild bergamot EO, containing thymol, is a potent antifungal agent against *Colletotrichum musae* and *Lasiodiplodia theobromae,* thereby controlling anthracnose and crown-rot diseases of banana fruits [23]. Moreover, the sustained release of thymol from metal–organic frameworks was shown to slow the growth of C. *musae* by two days compared to fruit treated without thymol [24]. The antifungal activity of thymol is attributable to different modes of action, including cell wall or membrane disruption, interference with ergosterol biosynthesis, reactive oxygen species generation, and lipid peroxidation in fungal cells, leading to a slower development of resistance in pathogens [25]. Thus, replacing synthetic antifungals and preservatives with thymol could be one viable option for preserving food and prolonging the shelf-life of fresh produce using a sustainable and non-toxic biopesticide. Although thymol has several beneficial properties, its application on a large scale in agriculture is limited due to low aqueous solubility, low stability, and high sensitivity to ultraviolet irradiation and elevated temperatures [26].

Encapsulation is a versatile approach to overcome the limitations of thymol as a potential postharvest antifungal agent. It is a process by which one material or a mixture (core) is coated with or entrapped within another material or system (wall), resulting in the formation of micro- or nanoparticles [27]. This technique offers further possibility for developing novel biopesticide formulations with potentially enhanced properties, controlled release, and improved stability [28, 29]. In recent years, various efforts have been made to develop green nanotechnology to reduce energy consumption, waste generation, and emissions of greenhouse gases. Using materials from renewable sources to fabricate nanocarrier systems can further contribute toward the development of green nanotechnology. Various nanocarrier systems of natural origin for developing botanical pesticides have recently gained prominence. Cenobio-Galindo et al. [30]. demonstrated that nanoemulsions of orange essential oils and xoconostle extract effectively controlled anthracnose growth, enhanced avocado firmness, and improved antioxidant activity due to the active compounds in the oils. Bill et al. [31] and Esquivel-Chavez et al. [32] reported that spray-dried thyme oil, encapsulated in modified starch/agave fructan microcapsules, effectively inhibited mycelial growth of Colletotrichum gloeosporioides and reduced anthracnose incidence in mangoes. Yegin et al. [33] showed that nanoencapsulation of geraniol essential oil in Pluronic F-127 nanoparticles not only prolonged the release of geraniol but also significantly inhibited the growth of *Escherichia coli* O157:H7 and *Salmonella enterica* both in vitro and on spinach surfaces. Additionally, Arcot et al. [34] demonstrated that nanoencapsulation of cinnamon bark essential oil in a hybrid of whey protein concentrate and food-grade wax nanoparticles significantly delayed the release of the essential oil, with an increased half-life of 61 h. This formulation also markedly reduced *S. aureus* and *E. coli* O157:H7 colony-forming units in vitro and effectively inhibited *Aspergillus flavus* mycelium, a common cause of black mold in red apples.

One attractive material for thymol encapsulation is zein, is a natural polymer found in maize that accounts for 45–50% of its protein. It has been recognized as a safe (GRAS) food additive, and has been studied for its potential to form low-cost, biocompatible, biodegradable films and hydrophobic coatings that can protect against microbial attack [35]. The amphipathic nature of zein enables it to interact with molecules of varying polarities and allows spontaneous self-assembly of nanoparticles and encapsulation of bioactive compounds in liquid – liquid dispersions [36]. These unique properties of zein make it an appealing nanoscale delivery system for fungicides and other agrochemicals. Several studies have shown that EO-loaded zein nanoparticles have potential postharvest applications as natural food preservatives. For instance, zein nanoparticles loaded with curcumin exhibited excellent antifungal properties against *Colletotrichum gloeosporioides,* suppressing anthracnose disease severity in mango fruit and thus preserving the food postharvest quality [37]. We therefore hypothesize that thymol encapsulated within a zein matrix could offer a promising candidate system to stabilize and deliver thymol to banana fruit post-harvest, thereby acting as an effective antifungal to enhance shelf-life during transportation, retail and consumer storage.

In this study, we aim to investigate the impact of zein encapsulation on the bioactivity of thymol against *C. musae*, demonstrating the nanoparticle system's potential for postharvest control of banana anthracnose. Our central hypothesis is that zein encapsulation enhances the antifungal efficacy of thymol by improving its stability and retention during application, in comparison to pure thymol. To test this, we characterize the fabricated zein nanoparticles in terms of morphology and thymol retention. We then assess and compare the antifungal activity of thymol-loaded zein nanoparticles with that of pure thymol. Ultimately, this work aims to demonstrate the potential of thymol-loaded zein nanoparticles as an effective component in a simple spray formulation for controlling postharvest decay in bananas, offering a promising alternative to traditional control methods for managing banana anthracnose.

2 Experimental section

2.1 Materials and equipment

Analytical grade ethanol, *n*-hexane, and ethyl acetate were used. Standard grade thymol was purchased from Fisher Scientific Company. *C. musae* was obtained from the Agricultural Biotechnology Laboratory, National Institute of Molecular Biology and Biotechnology, UPLB, Los Baños, Laguna, Philippines. Corn grits and Cavendish banana fruit were obtained from local suppliers in Los Baños, Laguna, Philippines.

2.2 Extraction of corn zein

Zein was extracted from milled corn grits using the modifications of previously reported methods [38–40]. Milled corn grits were soaked with shaking in 70% (v/v) aqueous ethanol at 60 °C for 24 h. The extract was concentrated using a rotary evaporator, added with water to precipitate crude zein, and centrifuged at 15,000 × *g* using Beckman Coulter Allegra X-30 Benchtop Centrifuge (Brea, CA, USA). Then, crude zein was redissolved in 95% (v/v) aqueous ethanol to obtain a 10% (w/v) solution, which was partitioned with equal volumes of *n*-hexane to remove fatty materials such as fatty acids, triacylglycerides, phytosterols, and phytosterol esters. Defatted zein was obtained by precipitation using distilled water and centrifugation at 15,000 × *g*. The defatted zein was washed with ethyl acetate several times to eliminate carotenoid pigments, continuing until the absorbance of the ethyl acetate washes at 450 nm (the absorbance maximum for lutein and zeaxanthin) reached a stable and approximately zero value. Lastly, the resulting material was air-dried to obtain the final zein extract as light-yellow solids. The final yield of zein extracted from dried corn grits was 6.99% (w/w). SDS-PAGE was used to evaluate the molecular weight and purity (presence or absence of non-zein proteins) of the zein isolate.

2.3 Preparation of thymol-loaded zein nanoparticles

Thymol-loaded zein nanoparticles were fabricated using a modified method of Mahalakshmi et al. [41] Zein and thymol were dissolved first in 70% (v/v) aqueous ethanol to obtain solutions with final concentrations of 50 g L^{-1} and 12.5 g L^{-1}, respectively. After combining equal volumes of zein and thymol solutions, the resulting mixture was added dropwise at a rate of 0.2 mL m^{-1} into two volumes of deionized water at 25 °C (maintained with a water bath) while stirring at 10,000 rpm using a Janke & Kunkel Ultra-turrax T50 homogenizer. The resulting dispersion was concentrated *in vacuo* and then lyophilized using a Labconco Freeze Dry System (Kansas City, MO, USA), yielding thymol-loaded zein nanoparticles as a light-yellow powder.

2.4 Characterization of thymol-loaded zein nanoparticles

2.4.1 Efficiency of encapsulation process

Parameters, indicating the efficiencies of the encapsulation process were determined using a modified method from previous reports [42–44]. Briefly, 10 mg of thymol-loaded zein nanoparticles were mixed with 1 mL 95% (v/v) ethanol and centrifuged at 15,000 × *g* to remove surface-bound thymol. The residue was collected, sonicated in 10 mL ethyl acetate for 1 h using a Cole Palmer bath sonication (53 kHz), and then centrifuged at 15,000 × *g*. The supernatant was collected and analyzed for thymol content by spectrophotometric quantification at 276 nm using a Shimadzu UVmini-1240 Scanning Spectrophotometer (Kyoto, JP) with thymol standard as control. Encapsulation efficiency, loading efficiency and payload were calculated using Eqs. 1, 2, and 3, respectively.

$$\text{Encapsulation efficiency}(\%) = \frac{\text{mass of entrapped thymol}}{\text{initial mass of thymol used}} \times 100 \quad (1)$$

$$\text{Loading efficiency}\ (\%) = \frac{\text{mass of entrapped thymol}}{\text{mass of nanoparticles}} \times 100 \quad (2)$$

$$\text{Payload}\ (\%) = \frac{\text{mass of entrapped thymol}}{\text{mass of wall materials}} \times 100 \quad (3)$$

2.4.2 Nanoparticle size and morphology

Atomic force microscopy (AFM) The protocol utilized for AFM imaging was adapted from a previous work [45]. To evaluate the morphology of thymol-loaded zein particles, about 10 mg of the dry powder was dispersed in 1.0 mL water, drop casted onto freshly cleaved mica film, air-dried, and then imaged using a Park Systems XE-70 Atomic Force Microscope (Suwon, South Korea) in non-contact mode with Nanosensors Point Probe Plus cantilever with a resonant frequency of 330 kHz and force constant of 42 N m^{-1}. Average particle diameters of at least 50 nanoparticles were measured by image analysis.

Transmission electron microscopy (TEM) TEM sample preparation and imaging protocol was adapted from a previous work [46]. Particle size and morphology of thymol-loaded zein particles were also studied using TEM (FEI Tecnai T20 TEM) at 200 keV. Samples were prepared by drop casting 3.0 µL aliquots of the particle dispersion onto a holey carbon film-coated, 300 mesh copper grid (EM Solutions), which was then air dried, prior to analysis. Average particle diameters of at least 50 nanoparticles were measured by image analysis.

Dynamic light scattering (DLS) and phase analysis light scattering (PALS) Methods for DLS and PALS is based on a recent work [47]. Size distribution and ζ-potential of the thymol-loaded zein particles were also determined by DLS and PALS, respectively. The dry sample powder was added with distilled, deionized water and the resulting aqueous dispersion was homogenized by sonication. The size distributions of the particles were determined by Brookhaven NanoBrook Omni particle sizer and zeta potential analyzer with a 35 mW red diode laser (λ = 640 nm; detection angle = 90°, and temperature = 25 °C). DLS and PALS were conducted three times independently ($n = 3$) with three measurements per sample.

2.4.3 Storage stability

The storage stability of thymol-loaded zein nanoparticles was evaluated using modified methods previously reported [42, 44, 48]. Dry powder samples (5 mg) were stored in sealed, 25-mL amber vials, one set of which was then placed in cold storage at 4 °C and another batch in ambient laboratory conditions at 25 °C for 40 d. At specific time points over the 40-d observation period, thymol contents of stored powders were quantified spectrophotometrically using the same method described in Sect. 2.4.1. Retention of thymol by the nanoparticles was calculated using Eq. 4.

$$\text{Retention } (\%) = \frac{\text{mass of entrapped thymol at time t}}{\text{initial mass of entrapped thymol}} \times 100 \tag{4}$$

2.5 Release Studies

Release of thymol from zein nanoparticles was evaluated using a previously reported dynamic dialysis method [39, 45]. Briefly, 2 g thymol-loaded zein nanoparticles in 10 mL release medium (0.3% (v/v) Tween® 80 in water) was loaded into a dialysis tubing (10 kDA molecular weight cut-off), sealed, and suspended in 90 mL of the same release medium. The external release medium was magnetically stirred at 300 rpm at 25 °C. At specific time points over 24 h, 1 mL of the external release medium was withdrawn and then replenished with an equal volume of fresh release medium. Thymol was quantified spectrophotometrically at 277 nm from the collected samples and the percentage cumulative thymol release was calculated. Release studies were conducted at least three times independently ($n = 3$).

Different release kinetics models [49, 50] were used to fit the release profile of thymol from zein nanoparticles, including the following:

$$\text{Zero} - \text{order} : Q_t = Q_0 + kt \tag{5}$$

$$\text{First} - \text{order} : Q_t = Q_0 - e^{-kt} \tag{6}$$

$$\text{Higuchi} : Q_t = kt^{1/2} \tag{7}$$

$$\text{Korsmeyer} - \text{Peppas} : Q_t = kt^n \tag{8}$$

$$\text{Hixson} - \text{Crowell} : {Q_t}^{1/3} = {Q_0}^{1/3} - kt \tag{9}$$

$$\text{Weibull} : Q_t = Q_\infty \left(1 - e^{(t/\tau)^\beta}\right) \tag{10}$$

where: Q_t is the amount of payload release at time t; Q_0 is the initial amount of released payload; k is the respective release rate constant of each model; n is the release exponent that indicates the mechanism of payload release ($n < 0.5$ for Fickian diffusion; $n = 0.5$ for anomalous diffusion; $0.5 < n < 1.0$ for case II transport; $n = 1.0$ for super case II transport; and $n > 1.0$ for non-Fickian release); Q_∞ is the total amount of payload that will be released; τ is the scale parameter that indicates the time scale of the release process; and β is the shape parameter, describing the release profile ($\beta < 1$ for a Fickian diffusion mechanism; $\beta = 1$ for a purely exponential process; and $\beta > 1$ for more complex release mechanisms, including erosion or degradation) [50].

2.6 Antifungal Assay: disc diffusion method

Antifungal activity of both non-encapsulated and encapsulated thymol against *C. musae* was determined using a modified method of Mukurumbira et al. [51] *C. musae* culture (100 µL) was evenly spread on potato dextrose agar (PDA) plates using sterile cotton swabs and incubated for 3 d to allow partial growth. Blank and sterile antimicrobial susceptibility discs (Whatman No. 1 filter paper, 5 mm diameter) were soaked in ethanolic solutions with different concentrations (0.5, 1, 2.5, and 5 g L^{-1}) of non-encapsulated thymol and thymol-loaded zein particles. It is important to note that the thymol contents of the thymol-loaded zein particles are lower (0.5, 1, 2.5, and 5 g nanoparticle L^{-1} solutions have equivalent thymol contents of 0.16, 0.31, 0.79, and 1.57 g L^{-1}, respectively). Then, discs were placed on the surface of the inoculated agar. Nystatin (1 g L^{-1}) and 70% (v/v) ethanol discs were used as the positive control and negative control, respectively. The fungal plates were then incubated at ambient room temperature (28 ± 2 °C) for 72 h. Inhibitory zone diameters were measured after incubation.

2.7 Antifungal assay on banana fruit

The antifungal activity of the thymol-loaded zein nanoparticles against *Colletotrichum musae*, the main pathogen of anthracnose, was assessed in detached Cavendish banana fruits (*Musa acuminata* AAA Subgroup) using a modification of previously reported protocols [42, 52]. Fruit samples from a local supplier in Los Baños, Laguna were harvested at the mature-green stage and were not subjected to any fungicide treatment. Fruits were sorted to fit the following selection criteria: (1) rot-free with minimal blemishes; and (2) relatively homogenous maturity and sizes. Within a few hours after harvesting, collected samples were dipped in 2% sodium hypochlorite to inactivate all the microorganisms on surfaces of the fruits, followed by rinsing with water, blot- and air-drying before inoculation. *C. musae* was inoculated by dipping each fruit into a spore suspension (5×10^4 spores mL^{-1}), followed by air-drying for approximately 2 h, prior to further treatment.

Solutions of non-encapsulated thymol and dispersions of zein-encapsulated thymol were prepared by dispersion into 70% (v/v) ethanol. Equal volumes of the liquid formulations (50 µg mL^{-1}) were then applied by spraying onto banana fruit. A positive control (untreated banana fruit) and negative control [70% (v/v) ethanol] were also included as a comparison. Treated fruits were then stored in different rooms under similar conditions at ambient temperature (25 ± 2 °C) for 10 d and were evaluated daily for the presence of symptoms of fungal activity (fungal growth, lesions, spots, and rot). After the storage period

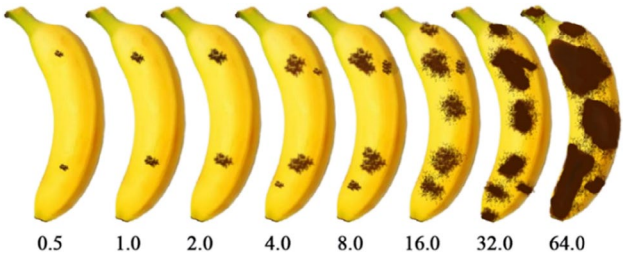

Fig. 1 Schematic diagram demonstrating different disease severity scores in bananas, corresponding to relative percentage of affected area per fruit [53]

of samples when fruits were fully yellow (C6 to C7 in the Von Loesecke scale), each fruit was assessed and scored according to the percentage of fruit skin areas covered with disease symptoms (depicted in Fig. 1) and the disease severity was calculated using Eq. 11. Disease severity was also assessed using digital image analysis applying Eq. 12, where the percentage of disease area was quantified relative to the total pixel area of the bananas in the images, employing ImageJ image processing software. All experiments were performed three times independently ($n = 3$) with three replicates for each treatment.

$$\text{Disease severity (\%)} = \frac{\Sigma \text{ disease area} \times \text{number of samples}}{\text{maximum rating} \times \text{total number of samples}} \times 100 \quad (11)$$

$$\text{Disease severity (\%)} = \frac{\text{pixel area of the disease site}}{\text{pixel area of banana sample}} \times 100 \quad (12)$$

2.8 AFM imaging of banana epidermis samples

Epidermis Sects. (10 mm × 20 mm × ~ 1 mm thick) were taken from treated and untreated banana epicarps (see Sect. 2.7 for treatment protocol) using a scalpel, placed onto clean glass slides, and imaged immediately to prevent wrinkling due to dehydration. Treated and untreated banana epidermis surfaces, as well as a thymol-loaded zein particle-treated glass slide (control), were imaged using a JPK Nanowizard 3 Atomic Force Microscope in intermittent contact (AC) mode with a Bruker NCHV cantilever (resonance frequency = 320 kHz; spring constant = 42 N m^{-1}; tip radius = 8 nm (nominal values)).

2.9 Statistical analysis

Statistical analyses were performed using GraphPad Prism v9.0 to assess the significance of the results. All data distributions were initially assessed for normality using the Shapiro–Wilk test. A significance level of $p < 0.05$ was set to determine statistical significance. One-way ANOVA evaluation was performed followed by multiple comparison

test. All data presented are expressed as mean ± standard deviation (SD).

3 Results and Discussion

3.1 Fabrication of thymol-loaded zein nanoparticles

3.1.1 Characteristics of corn zein

Zein was obtained as a pale-yellow powder from finely ground corn grits, with a yield of 6.99% (w/w). The extraction method utilized was specifically designed to yield pure zein. This is supported by SDS-PAGE analysis (Fig. S1), which shows that the extracted zein is predominantly composed of α-zeins (20–25 kDa, major component) and γ-zein (α-zein dimers, ~ 50 kDa, minor component), devoid of non-zein proteins [54, 55]. The zein extract also exhibited a high emulsifying activity and stability ~ 90% (Fig. S1), similar to previous studies on zein [56, 57]. Zein's secondary structure contains more than 50% α-helix arranged in segments of equal length, which have hydrophobic surfaces, [58] giving rise to a ribbon-like tertiary structure with sharply defined hydrophobic and hydrophilic domains that enable zein to function as a polymeric amphiphile [59]. The observed emulsifying properties can be attributed to these hydrophilic and hydrophobic domains, which allow zein to adsorb strongly at and stabilize interfaces of immiscible liquids [60]. From a practical viewpoint, zein is an highly versatile and ideal material for developing packaging nanocomposites, antimicrobial colloidal systems, and oral route delivery systems, as it is readily available, renewable, and classified as a GRAS and food-grade ingredient, [61] in addition to its odorless and tasteless characteristic, biodegradability, biocompatibility, and unique solubility behaviors [62]. These characteristics make zein an ideal choice as an encapsulating agent for encapsulation of bioactives, particularly water-insoluble and oil-based actives, leading to stable and finely dispersed nanoparticles or emulsion nanodroplets.

3.1.2 Nanoencapsulation of thymol using corn zein

In this section of the study, thymol was encapsulated in zein using a modified emulsification method, [41] as presented in the schematic diagram in Fig. 2a. This method is based on manipulation of the unique solubility characteristics of zein in different aqueous ethanolic systems. Initially, thymol and zein (2:5 mass ratio) were dissolved in 70% (v/v) aqueous ethanol—zein is soluble in 60–90% (v/v) aqueous ethanol solution [63] —followed by emulsification via high-speed shearing to produce liquid nanodroplets. This simple technique is known as antisolvent precipitation, which involves dropping a zein-containing organic solution into an aqueous ethanolic solution, allowing zein molecules to assemble into thymol-loaded particles. This zein nanoparticle preparation technique has been recognized as an effective delivery system for hydrophobic bioactive compounds [64]. The succeeding *in vacuo* drying step reduces the ethanol content in the mixture, causing the formation of thymol-loaded zein nanoparticles [65]. Lyophilization of the resulting mixture yielded thymol-loaded zein nanoparticles as a light-yellow powder with 89.32% (w/w) yield.

A high encapsulation efficiency (EE) of 70% was observed, indicating that zein effectively entrapped the thymol core within the nanoparticles. Typical encapsulation efficiencies of zein nanocarriers with hydrophobic payloads in previous reports range from 50–70% [66, 67]. Loading efficiency and payload, which are important parameters in dose calculations, are presented in Table S1 in the Electronic Supporting Information.

3.2 Size and morphology of thymol-loaded zein nanoparticles

Based on the DLS data (Fig. 2b), thymol-loaded zein nanoparticles had a unimodal hydrodynamic size distribution with an effective diameter of 300 nm and a polydispersity index of 0.337. PALS analysis revealed that the particles had a ζ-potential of –32 mV, indicating a highly negative surface charge, imparting good colloidal stability in dispersion (*i.e.,* particles will not aggregate easily in dispersion). To confirm the measured size and study the morphology of thymol-loaded zein nanoparticles, samples were imaged via AFM and TEM. AFM (Fig. 2c and d) and TEM images (Fig. 2e and f) revealed that the nanoparticles were highly dispersible particles, exhibiting good size agreement with DLS measurement (average diameters: 285 ± 29 nm for AFM and 290 ± 34 nm for TEM). Furthermore, the particles have an overall spherical morphology and a smooth interface. The consistent electron density throughout each nanoparticle, represented by Fig. 2f, denotes that the system is a matrix-type particle, wherein thymol is uniformly dispersed within the zein matrix. The size range and uniformity of the particle in TEM corroborate with the observed values in DLS and are similar to the sizes reported in the literature for nanoparticles produced with zein through the same encapsulation method [68, 69].

3.3 Storage stability of thymol-loaded zein nanoparticles

The efficacy of thymol retention within the nanoparticles was evaluated at specific time points during a 40-d

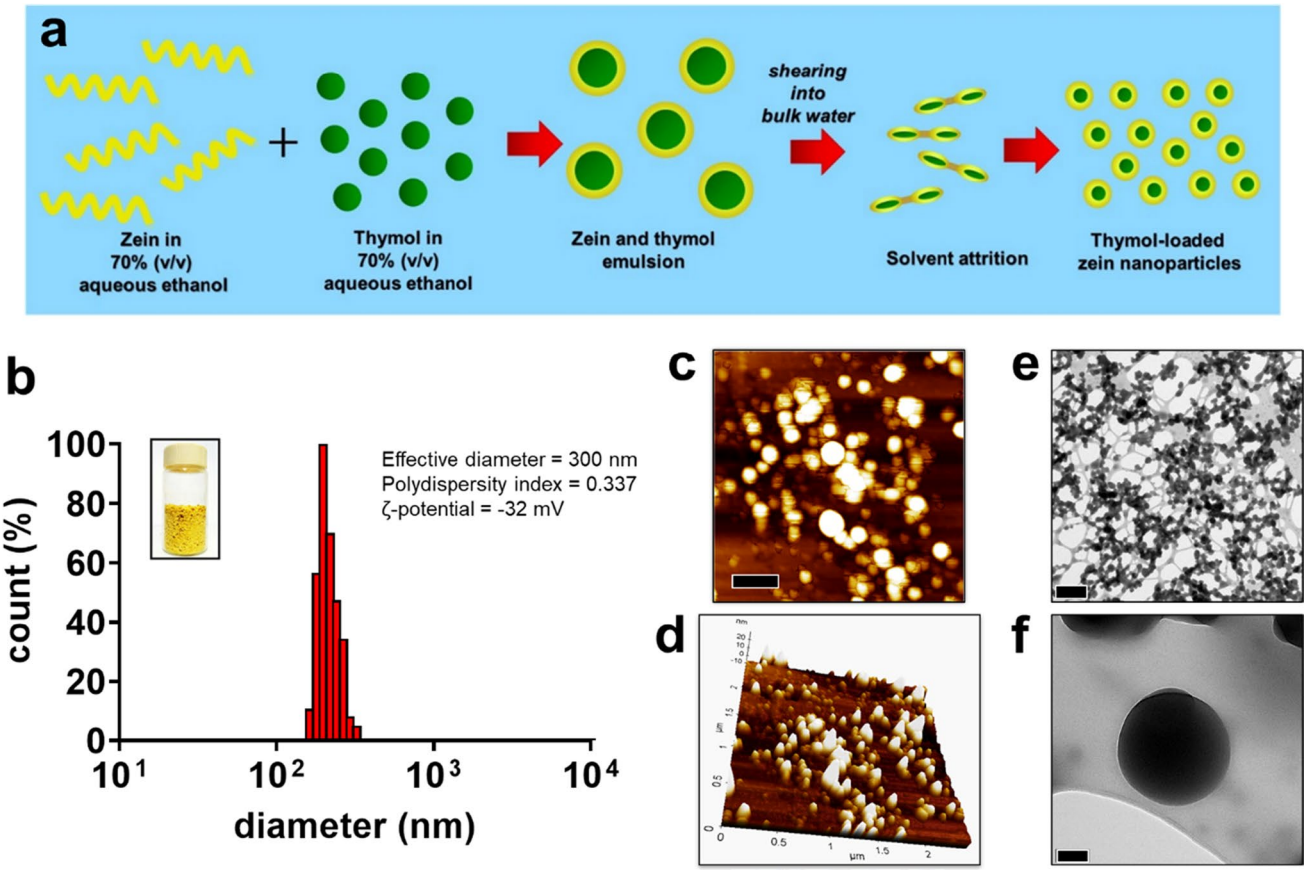

Fig. 2 **a** Schematic representation of the fabrication process of thymol-loaded zein nanoparticles. **b** Size distribution of thymol-loaded zein nanoparticles based on dynamic light scattering analysis. The inset shows a photograph of the nanoparticles in dry powder form. **c** Atomic force microscopy image and **d** its three-dimensional projection showing the smooth spherical morphology of thymol-loaded zein nanoparticles. **e** and **f** Representative transmission electron micrographs of thymol-loaded zein nanoparticles. Scale bars = **c** 300 nm, **e** 1.5 µm, and **f** 100 nm

storage period at two different storage conditions: 4 °C (refrigerated) and 25 ± 2 °C (ambient laboratory conditions). As shown in Fig. 3, thymol-loaded zein nanoparticles exhibited a gradual decrease in thymol retention over the storage period. A more rapid decline with a significant drop in thymol retention was observed in samples stored at 25 °C as early as day 15, while samples stored at 4 °C only showed a significant decline in thymol retention starting on day 35. Consequently, the final thymol retention was lower in samples at room temperature after 40 d. Overall, thymol was effectively retained within the zein nanoparticles under both storage conditions with final thymol retentions of 97.4 ± 0.3% (25 °C) and 98.3 ± 0.3% (4 °C). Although there is a minor difference in final thymol retention between the two storage conditions, the high retention of thymol by the zein nanoparticles, even at room temperature, demonstrates capability of zein encapsulation system to entrap and stabilize thymol across various storage environments.

3.4 Release profile of thymol from zein nanoparticles

The release behavior of thymol from zein nanoparticles was assessed in aqueous environment using a dynamic dialysis method. In this approach, thymol-loaded zein nanoparticles were dispersed in the release medium and then loaded into sealed dialysis membrane 'bags' and suspended in fresh release medium. The dialysis membranes had molecular weight cut-off of 10 kDa, which is smaller than the size of α-zein (20–25 kDa). This configuration allowed for the diffusion of released thymol molecules into the external release medium while preventing the thymol-loaded zein nanoparticles (and potentially eroded α-zein) from mixing with the release phase. The release medium also contained 0.3% (v/v) Tween® 80 to enhance the solubilization of released thymol, facilitating straightforward quantification of the released compound.

The release pattern of thymol from zein nanoparticles is shown in Fig. 3b. A rapid release is observed in the aqueous

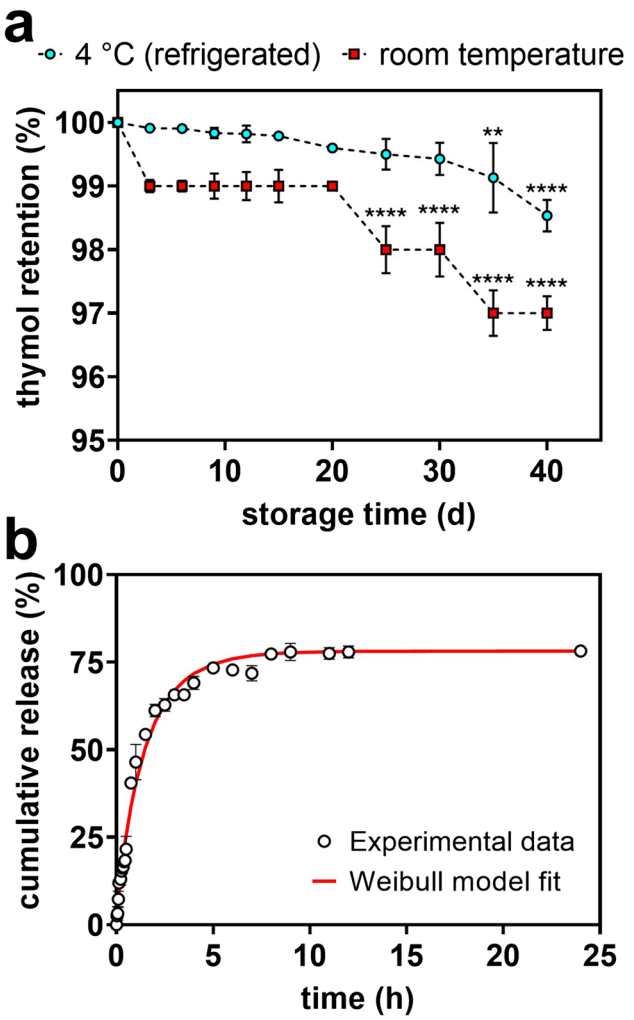

Fig. 3 **a** Thymol retention of thymol-loaded zein nanoparticles at 4 °C (refrigerated, blue-filled circles) and at ambient room temperature conditions (25 ± 2 °C, red-filled squares) over a 40-d storage period. Mean ± SD from three independent experiments ($n = 3$); $^{**}p < 0.01$, $^{****}p < 0.0001$ by one-way ANOVA with multiple comparisons vs thymol retention at t = 0 d. **b** Release profile of thymol from zein nanoparticles in aqueous medium over 24 h and the Weibull model fitting of the release data

medium during the first two hours, followed by a slower release rate up to the eighth hour. From 8 to 24 h, the release of thymol stabilizes at approximately 78% of the total encapsulated amount. To gain insights into this release behaviour and the possible mechanisms, various release kinetics models were used to fit the release data, including: zero-order, first-order, Korsmeyer–Peppas, Hixon–Crowell, Higuchi, and Weibull models. The derived parameters and correlation coefficients (R^2) are summarized in Table 1. In previous recent works, the Korsmeyer–Peppas model have accurately captured the release behaviors of many different types of payloads from zein nanoparticles [70–72]. In our case, the Weibull model fits reasonably well with the experimental release pattern with the highest R^2 value (Table 1). This model is particularly valuable for studying the drug release profiles of matrix systems, [49] and hence are particularly suited for zein nanoparticles in this work as they are matrix-type systems (See TEM images in Fig. 2e and f). The derived parameters from this model are the timescale parameter ($\tau = 1.43$ h), which represents the characteristic time at which significant drug release occurs, and the shape parameter ($\beta = 0.89$), which describes the overall profile of the release pattern. Recent work by de Jesus Martin-Camacho et al. [73] established a correlation between the Korsmeyer–Peppas release exponent n and the Weibull shape parameter β. According to their findings, the β of 0.89 (in this work) falls in range $0.56 < \beta < 1.08$, which corresponds to a Korsmeyer–Peppas n value range of $0.43 < n < 0.85$. This indicates an anomalous transport mechanism for spherical matrix-type polymeric particles. This release behavior is likely influenced by complex interactions among the medium, the zein matrix, and thymol payload, as well as by multiple simultaneous processes, possibly including diffusion, swelling, relaxation, or erosion, often leading to an initial rapid release phase into aqueous environments followed by slower release rate that may eventually approach a steady state.

Table 1 Calculated parameters and correlation coefficients of fitting different release kinetics models to the release profile of thymol from zein nanoparticles in aqueous environment

Model	Derived parameters*	R^2
Zero-order	$k = 3.75$	0.498
First-order	$k = 0.26$	0.610
Higuchi	$k = 20.8$	0.780
Hixson–Crowell	$k = 0.11$	0.407
Korsmeyer–Peppas	$k = 0.37$; $n = 0.53$	0.906
Weibull	$\tau = 1.43$; $\beta = 0.89$	0.989

*k = release rate constant for specific models (zero- and first-order, Higuchi, and Hixson–Crowell); n is the Korsmeyer–Peppas release exponent; τ is the Weibull timescale parameter; and β is the Weibull shape parameter

3.5 Antifungal activity of thymol-loaded zein nanoparticles

3.5.1 *In vitro* activity against *C. musae*

The antifungal activity of non-encapsulated thymol and thymol-loaded zein nanoparticles was tested against *C. musae* using a disc diffusion assay. *C. musae* as the main causative pathogen of anthracnose, the most widely spread disease of bananas in tropical regions. It is also the causal agent of crown rot, stem-end rot, and blossom-end rot in bananas [74]. In this study, thymol was chosen as the model antifungal as it is a ubiquitous component in many plant-derived bioactives, making it an easy-to-source natural alternative

to synthetic fungicides. Thymol and other monoterpenoids are efficient antifungal agents against *Colletotrichum* species via the following mechanisms: interference with cell membrane integrity and suppression of pump efflux, which were demonstrated in a previous study [75].

The results of the disc diffusion assay are summarized in Fig. 4 and Fig. S3 in the Electronic Supporting Information. At the lowest test concentration (0.5 g L^{-1}), both non-encapsulated thymol and thymol-loaded zein nanoparticles (thymol content: 0.16 g L^{-1}) showed no zone of inhibition, similar to the solvent or vehicle control (70% ethanol). Increased antifungal activity was observed at non-encapsulated thymol concentrations range of 1 to 5 g L^{-1}; however, a leveling effect (*i.e.*, no significant change in inhibitory activity) was observed at this range, despite the five-fold concentration increment. On the other hand, thymol-loaded zein nanoparticles showed increasing antifungal activity with the two highest concentrations (2.5 and 5 g L^{-1} with equivalent thymol concentrations of 0.79 and 1.57 g L^{-1}, respectively), comparable to the nystatin standard.

Comparison of non-encapsulated thymol and thymol-loaded zein nanoparticles (Fig. S3 in the Electronic Supporting Information) showed no significant difference in the activities at the concentration range of 0.5 to 2.5 g L^{-1}. Thymol-loaded zein nanoparticles at 5 g L^{-1} showed significantly higher activity than non-encapsulated thymol and thymol-loaded zein nanoparticles at lower concentrations. It should be noted, however, that the thymol content of the zein nanoparticles is lower (~ 30% w/v thymol content) than non-encapsulated thymol treatments. Considering the thymol content of the nanoparticles and the observed antifungal activity, encapsulation of thymol within the zein nanoparticles significantly enhanced the percentage antifungal activity of thymol by around 200- to 300-fold. Thymol is a volatile compound, and its increased activity can be attributed to its modulated release and diffusion from zein nanoparticles, allowing it to exert its antifungal effects even at lower concentrations.

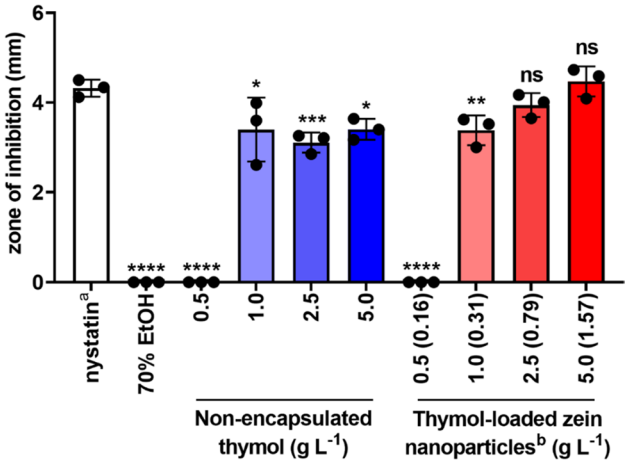

Fig. 4 Zones of inhibition at different concentrations of non-encapsulated and encapsulated thymol, 70% ethanol (solvent control), nystatin (antifungal standard) against *Colletotrechum musae*. [a]Nystatin concentration = 1 g L^{-1}. [b]Thymol concentrations of the nanoparticles are indicated in parentheses. Data presented as Mean ± SD ($n = 3$ independent experiments). ****$p < 0.0001$, ***$p < 0.001$, **$p < 0.01$, *$p < 0.1$, *ns* not significant, by one-way ANOVA with multiple comparisons vs nystatin. Multiple comparisons between all samples are shown in Fig. S3 in the Electronic Supporting Information

3.5.2 Postharvest control for banana anthracnose

The performance of thymol-loaded zein nanoparticles as a postharvest control for anthracnose was evaluated on C. *musae*-infected banana fruits for 10 d, which covers the ripening period of bananas. Representative photographs demonstrating the changes in the appearance of untreated and treated banana fruit and the emergence of disease symptoms are shown in Fig. 5a. Representative photographs of some anthracnose symptoms are also shown in Fig. 5b and c.

Based on the observations, untreated and solvent-treated bananas (70% ethanol—solvent or dispersant control) exhibited black, sunken spots, indicating fungal growth, upon ripening on day 2. Both encapsulated (thymol-loaded zein nanoparticles) and non-encapsulated thymol significantly prevented the appearance of small black and brown bruises, which were prominent in untreated and solvent-treated bananas from days 6. Thymol-loaded zein nanoparticle treatment was able to delay the appearance of white fungal growth on the bananas' crown-tip and body, symptoms that first appeared in untreated and solvent-treated bananas on day 6. Moreover, thymol-loaded zein nanoparticles delayed black fungal growth on the bananas' crown tip and body—observed only from day 9. In comparison, the first appearance of these symptoms is earlier in untreated and solvent-treated bananas (day 2) and in non-encapsulated thymol-treated bananas (day 7). Black fungal growth on the banana fingertips was not observed in thymol-loaded zein nanoparticle-treated bananas, whereas untreated, solvent-treated, and non-encapsulated thymol-treated bananas showed signs of disease on day 8. Interestingly, samples treated with free thymol and thymol-loaded zein nanoparticles exhibited a delay in ripening (about one to two days later) as compared to the controls. After the 10-d observation period, free thymol- and encapsulated thymol-treated samples have better overall quality, in comparison to the untreated and solvent-sprayed groups.

The performance of thymol-loaded zein nanoparticles to combat anthracnose in bananas was also evaluated using disease severity scores at day 10, as shown in Fig. 5d. Both thymol-loaded zein nanoparticle and free thymol (non-encapsulated) treatment significantly reduced disease severity by 50–60%, in comparison to the untreated and solvent-treated

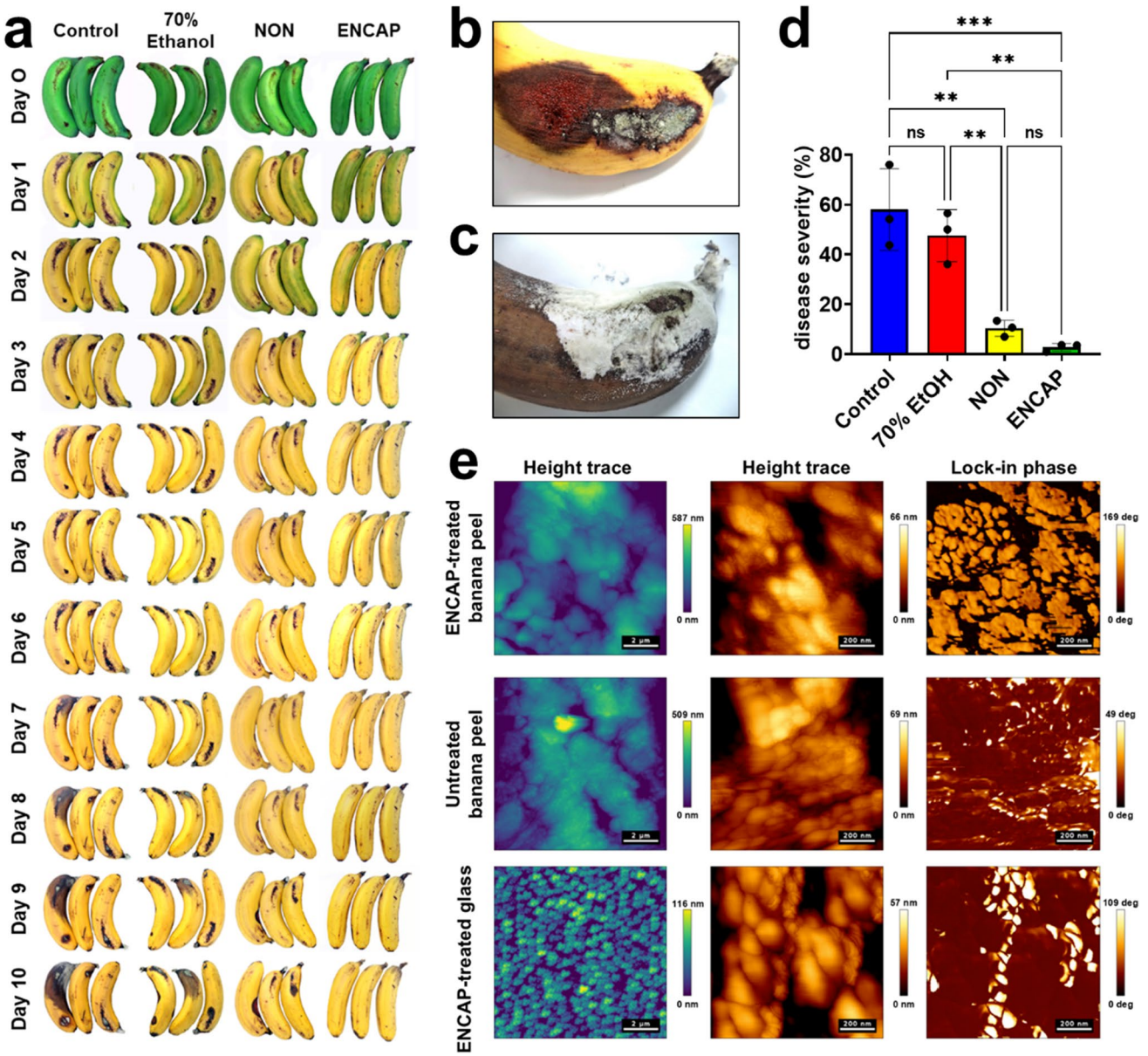

Fig. 5 **a** Representative photographs showing the different maturity stages of and various degrees of fungal attack on Cavendish banana fruit with different treatment – control (untreated bananas, negative control), 70% ethanol (70% EtOH, solvent control), non-encapsulated thymol (NON) and thymol-loaded zein nanoparticles (ENCAP) – over 10 d of storage. Photographs showing the **b** red and **c** white fungal growth on banana fruit. **d** Disease severity data on banana fruits with different treatments at day 10. Data presented as Mean ± SD ($n = 3$ independent experiments). $****p < 0.0001$, $**p < 0.01$, *ns* not significant, by one-way ANOVA with multiple comparisons between all samples. **e** Representative AFM images of untreated and thymol-loaded zein nanoparticle (ENCAP)-treated Cavendish banana fruit epidermis, and ENCAP-treated glass surface (control). *Left* and *middle* column images are height traces (low and high magnification, respectively) with color bars showing relative sample heights of scanned surfaces. *Right* column images are lock-in phase images with color bars showing phase angles of scanned surfaces. Scale bars = (**e**, *left panel*) 2 µm and (**e**, *middle* and *right panels*) 200 nm

groups. Notably, thymol-loaded zein nanoparticle-treated samples exhibited significantly lower disease severity scores, compared to non-encapsulated thymol groups, indicating the improvement performance of thymol in the encapsulated form against the progression of anthracnose in bananas.

The observed bioactivity of thymol-loaded zein nanoparticles can be mainly attributed to the enhanced antifungal activity of thymol due to nanoencapsulation and their capability to form nanoparticle-rich surface coatings when applied as a spray component. A representative photomicrograph in Fig. S4 demonstrates the resulting thin film from spraying the ethanolic dispersion of thymol-loaded zein nanoparticle formulation. To further demonstrate and characterize this capability, surface topology and properties

of the epidermis from spray-treated and untreated banana epicarps were explored using AFM imaging. Height trace AFM images of both the thymol-loaded zein nanoparticle-treated and untreated banana epidermis (Fig. 5e and Fig. S5) depict the inherently rough structure of the epidermis surfaces similar to structures observed in previous reports. The untreated epidermis features numerous spherical to ellipsoidal microaggregates and nanograins of epicuticular wax with three distinct size populations: 127 ± 24 nm, 317 ± 102 nm and 673 ± 92 nm in diameter. In contrast, the treated epidermis shows these waxy structures interspersed with subtle film-like nanoscopic features, which are most likely arising from the deposition of the nanoparticles in between the wax grains. These indicate that the rough structure of the epidermis facilitates the entrapment and deposition of thymol-loaded zein nanoparticles onto the banana fruit epidermis.

Due to the similarity of the size and morphology of the thymol-loaded zein nanoparticles with the epicuticular wax grains, distinguishing between them in the AFM images is challenging. Fortunately, lock-in phase AFM images (Fig. 5e, *right panel*) highlight distinct differences in phase angles between the treated and untreated surfaces. The phase angle of the thymol-loaded zein nanoparticle-treated surfaces is $168 \pm 1°$, which is much higher than the $55 \pm 12°$ observed for untreated surfaces. This phase angle is also closer to that of the control glass slide coated with thymol-loaded zein nanoparticles ($125 \pm 25°$). These results confirm that the thymol-loaded zein nanoparticles effectively form a film layer and coat the banana fruit epidermis.

Furthermore, AFM imaging of the coating edge (Fig. S5), where some uncoated epidermis is exposed, reveal that the coating is thicker due to the 'coffee ring effect.' In this area, rather than observing a film coating between the wax grains, the grains themselves appear to be fully coated and exhibit a smoother surface. Moreover, the smaller nanograins in the untreated epidermis (127 ± 24 nm and 317 ± 102 nm in diameter) are less discernible, while the larger grains show an increased average size of 911 ± 121 nm compared to 673 ± 92 nm in the untreated samples. These findings strongly support the conclusion that the banana epidermis is effectively covered with thymol-loaded zein nanoparticles.

The physical properties of zein and the nanoparticle system and the bioactivity of thymol exhibit a synergistic effect on preserving the integrity of treated bananas during storage. Thymol is a volatile compound that does not remain effective for long if unencapsulated. However, the zein film-forming process traps thymol on the banana epidermis, significantly extending its presence and activity. This encapsulation allows thymol to remain active for a longer duration, enhancing its antifungal efficacy. The storage experiments demonstrated the inherent antifungal activity of thymol against *C. musae*, as supported by the in vitro antifungal activity experiments. This bioactivity is further enhanced by the zein nanoparticles' ability to effectively retain thymol and release it upon contact with water, as demonstrated by the in vitro release experiments. Moreover, the disease susceptibility was reduced by the delayed ripening of the fruit, caused by the hydrophobic nature of thymol and the film-forming capability of zein. Important to note that anthracnose gives latent fruit infection, *i.e.*, symptoms do not appear until the fruit is ripe [76]. A thin film of thymol-loaded zein nanoparticles provided a coating on the fruit peels' epidermis, which could potentially prevent ethylene diffusion and delay fruit ripening, as supported by previous reports [77, 78]. Furthermore, the thin film embedded with antifungal thymol-loaded zein nanoparticles can also interfere with fungal cell growth via limiting gas diffusion, which is essential for aerobic *C. musae*. Overall, thymol-loaded zein nanoparticles offer potential alternatives and possibly a new class of materials for food preservation and postharvest treatment; as such, the demonstrated properties and mechanisms in this work warrant further exploration and innovations in future works.

4 Conclusions

This study successfully demonstrated the fabrication of a highly dispersible and efficient antifungal thymol-loaded zein nanoparticle system. The developed nanoparticles exhibited exceptional thymol encapsulation efficiency and retained high thymol loading even after storage under various conditions. Moreover, our findings revealed a remarkable enhancement in the in vitro antifungal activity against *C. musae*, the primary cause of banana anthracnose. Importantly, when these thymol-loaded zein nanoparticles were utilized as a spray component for banana postharvest treatment, they effectively prevented or delayed the onset of symptoms associated with banana anthracnose.

These results highlight the potential of nanoparticle systems to serve as an innovative solution for fruit preservation by employing volatile but potent bioactive. By designing and fabricating such nanoparticle systems, we can harness and improve their antifungal properties and effectively combat postharvest diseases. The successful application of the thymol-loaded zein nanoparticles in preventing or delaying banana anthracnose demonstrates their promise as a viable antifungal treatment.

Overall, this study contributes to the growing body of research on nanotechnology-based approaches for agricultural applications, particularly in the field of fruit preservation. The development of nanoparticle systems offers a new avenue for the design of effective antifungal treatments, and further investigations are warranted to explore their potential in other fruit and postharvest diseases. The findings presented here pave the way for the development of sustainable and environmentally friendly strategies to improve the quality and shelf life of fruit while reducing the reliance on conventional chemical treatments.

Supplementary Information The online version contains supplementary material available at https://doi.org/10.1007/s42247-024-00851-6.

Acknowledgements The authors acknowledge the technical support and use of instruments and resources from the following institutions and individuals: UPLB Nanotechnology Analytical and Instrumentation Service Laboratory and the UPLB Nanobiotechnology Laboratory, headed by Dr. Lilia M. Fernando; Dr. Cuong Viet Pham and Mr. Yuyang Song, as well as the resources made available within the Molecular Imaging and Molecular Imaging and Theranostics Lab (headed by Prof. Xiaowei Wang) at the Baker Heart and Diabetes Institute; and the Soft Materials and Colloids (SMaC) Lab, School of Chemistry, Monash University. The authors also acknowledge the use of equipment within the Monash Centre for Electron Microscopy (MCEM), a Node of Microscopy Australia.

Author contributions All authors contributed to the study conception and design. Material preparation, data collection and analysis were performed by Dana C. Punelas–Villanueva, Ronaniel A. Almeda, Mari Sherlin Salisi–Chua, Rico F. Tabor, and Mark Louis P. Vidallon. Materials and resources were provided by Rico F. Tabor and Evelyn B. Rodriguez. The first draft of the manuscript was written by Dana C. Punelas–Villanueva, Ronaniel A. Almeda, and Evelyn B. Rodriguez. All authors commented on previous versions of the manuscript. All authors read and approved the final manuscript.

Funding Open Access funding enabled and organized by CAUL and its Member Institutions.

Data Availability Data available on request from the authors.

Declarations

Competing Interests The authors declare that they have no known competing financial interests or personal relationships that could have appeared to influence the work reported in this paper.

References

1. M.A.A. Mangoba, D.G. de Alvindia, Fungicidal activities of Cymbopogon winterianus against anthracnose of banana caused by Colletotrichum musae. Sci. Rep. **13**, 6629 (2023)
2. M. Kumari, et al., Chapter 14 - Microbial formulation approaches in postharvest disease management. in *Food Security and* Plant *Disease Management* (eds. Kumar, A. & Droby, S.) (Woodhead Publishing, 2021), p. 279–305. https://doi.org/10.1016/B978-0-12-821843-3.00007-6
3. F. Lopez-Galvez, P. Ragaert, L.A. Palermo, M. Eriksson, F. Devlieghere, Effect of new sanitizing formulations on quality of fresh-cut iceberg lettuce. Postharvest Biol. Technol. **85**, 102–108 (2013)
4. A. Landfeld et al., Decontamination of cut carrot by Persteril® agent based on the action of peroxyacetic acid. Czech. J. Food. Sci. **28**, 564–571 (2010)
5. A. Ali, M.K. Ong, C.F. Forney, Effect of ozone pre-conditioning on quality and antioxidant capacity of papaya fruit during ambient storage. Food Chem. **142**, 19–26 (2014)
6. P.V. Mahajan, O.J. Caleb, Z. Singh, C.B. Watkins, M. Geyer, Postharvest treatments of fresh produce. Philos. Trans. R. Soc. A Math. Phys. Eng. Sci. **372**, 20130309 (2014)
7. M. Ghasemnezhad, S. Zareh, M. Rassa, R.H. Sajedi, Effect of chitosan coating on maintenance of aril quality, microbial population and PPO activity of pomegranate (Punica granatum L. cv. Tarom) at cold storage temperature. J. Sci. Food Agric. **93**, 368–374 (2013)
8. M. Palumbo et al., Emerging postharvest technologies to enhance the shelf-life of fruit and vegetables: An obverview. Foods **11**, 3925 (2022)
9. X. Zhang, B. Li, Z. Zhang, Y. Chen, S. Tian, Antagonistic yeasts: A promising alternative to chemical fungicides for controlling postharvest decay of fruit. J. Fungi. **6**, 158 (2020)
10. C. Vischetti et al., Effectiveness of four synthetic fungicides in the control of post-harvest gray mold of strawberry and analyses of residues on fruit. Agronomy **14**, 65 (2024)
11. P.M. Ngegba, G. Cui, M.Z. Khalid, G. Zhong, Use of botanical pesticides in agriculture as an alternative to synthetic pesticides. Agriculture **12**, 600 (2022)
12. F.E. Mukah, P.A. Chinedu-Ndukwe, O. Imarhiagbe, D.A. Nwaubani, Agrochemical Use and Emerging Human and Animal Diseases. in *One Health Implications of Agrochemicals and their Sustainable Alternatives* (eds. Ogwu, M. C. & Chibueze Izah, S.) (Springer Nature, Singapore, 2023), p. 53–76. https://doi.org/10.1007/978-981-99-3439-3_2.
13. D.D. Bhutia, Y. Zhimo, R. Kole, J. Saha, Antifungal activity of plant extracts against Colletotrichum musae, the post harvest anthracnose pathogen of banana cv. Martaman. Nutr. Food. Sci. **46**, 2–15 (2016)
14. I.-H. Kim, Y.A. Oh, H. Lee, K.B. Song, S.C. Min, Grape berry coatings of lemongrass oil-incorporating nanoemulsion. LWT Food Sci. Technol. **58**, 1–10 (2014)
15. G. Gundewadi, S.G. Rudra, D.J. Sarkar, D. Singh, Nanoemulsion based alginate organic coating for shelf life extension of okra. Food Packag. Shelf LifePackag. Shelf. Life. **18**, 1–12 (2018)
16. N. Robledo, L. López, A. Bunger, C. Tapia, L. Abugoch, Effects of antimicrobial edible coating of thymol Nanoemulsion/Quinoa Protein/Chitosan on the safety, sensorial properties, and quality of refrigerated strawberries (Fragaria × ananassa) under commercial storage environment. Food Bioprocess Technol. **11**, 1566–1574 (2018)
17. R. Severino et al., Antimicrobial effects of modified chitosan based coating containing nanoemulsion of essential oils, modified atmosphere packaging and gamma irradiation against *Escherichia coli* O157:H7 and *Salmonella* Typhimurium on green beans. Food Control **50**, 215–222 (2015)
18. M. Miranda et al., Nano- and Micro- Carnauba Wax Emulsions versus Shellac Protective Coatings on Postharvest Citrus Quality. (2021). https://doi.org/10.21273/JASHS04972-20
19. L. Buendía−Moreno et al., Active cardboard box with a coating including essential oils entrapped within cyclodextrins and/or halloysite nanotubes. A case study for fresh tomato storage. Food Control **107**, 106763 (2020)
20. A. Kowalczyk, M. Przychodna, S. Sopata, A. Bodalska, I. Fecka, Thymol and thyme essential oil—new insights into selected therapeutic applications. Molecules **25**, 4125 (2020)

21. J. Ding et al., Effects of thymol concentration on postharvest diseases and quality of blueberry fruit. Food Chem. **402**, 134227 (2023)
22. S. Lee, H. Kim, L.R. Beuchat, Y. Kim, J.-H. Ryu, Synergistic antimicrobial activity of oregano and thyme thymol essential oils against *Leuconostoc citreum* in a laboratory medium and tomato juice. Food Microbiol.Microbiol. **90**, 103489 (2020)
23. S.A. Kulkarni, P.S. Sellamuthu, S.K. Nagarajan, T. Madhavan, E.R. Sadiku, Antifungal activity of wild bergamot (*Monarda fistulosa*) essential oil against postharvest fungal pathogens of banana fruits. S. Afr. J. Bot. **144**, 166–174 (2022)
24. J. Zuniega et al., Encapsulation of thymol and limonene in metal–organic frameworks for inhibition of Colletotrichum musae growth. Int. J. Food Sci. Technol. **59**, 730–742 (2024)
25 L. Shcherbakova et al., Studying the ability of thymol to improve fungicidal effects of tebuconazole and difenoconazole against some plant pathogenic fungi in seed or foliar treatments. Front. Microbiol.Microbiol. **12**, 6294229 (2021)
26. A. Hajibonabi et al., Antimicrobial activity of nanoformulations of carvacrol and thymol: New trend and applications. OpenNano **13**, 100170 (2023)
27. N. Vasisht, Chapter 15 - Nanoencapsulation in the food industry. in Microencapsulation in the Food Industry (Academic Press), pp. 209–213 (2023)
28. M. Bae et al., Novel biopesticides based on nanoencapsulation of azadirachtin with whey protein to control fall armyworm. J. Agric. Food Chem. **70**, 7900–7910 (2022)
29. Z. Milićević et al., Encapsulated clove bud essential oil: a new perspective as an eco-friendly biopesticide. Agriculture **12**, 338 (2022). https://doi.org/10.3390/agriculture12030338
30. A.J. de Cenobio-Galindo et al., Influence of bioactive compounds incorporated in a nanoemulsion as coating on avocado fruits (Persea americana) during postharvest storage: Antioxidant activity, physicochemical changes and structural evaluation. Antioxidants **8**, 500 (2019)
31. M. Bill, L. Korsten, F. Remize, M. Glowacz, D. Sivakumar, Effect of thyme oil vapours exposure on phenylalanine ammonia-lyase (PAL) and lipoxygenase (LOX) genes expression, and control of anthracnose in 'Hass' and 'Ryan' avocado fruit. Sci. Hortic.Hortic. **224**, 232–237 (2017)
32. F. Esquivel-Chávez et al., Control of mango decay using antifungal sachets containing of thyme oil/modified starch/agave fructans microcapsules. Future. Foods. **3**, 100008 (2021)
33. Y. Yegin, K.L. Perez-Lewis, M. Zhang, M. Akbulut, T.M. Taylor, Development and characterization of geraniol-loaded polymeric nanoparticles with antimicrobial activity against foodborne bacterial pathogens. J. Food Eng. **170**, 64–71 (2016)
34. Y. Arcot et al., Edible nano-encapsulated cinnamon essential oil hybrid wax coatings for enhancing apple safety against food borne pathogens. Curr. Res. Food. Sci. **8**, 100667 (2024)
35. A.C. Jaski et al., Zein - a plant-based material of growing importance: New perspectives for innovative uses. Ind. Crops Prod. **186**, 115250 (2022)
36. X. Yan, M. Li, X. Xu, X. Liu, F. Liu, Zein-based nano-delivery systems for encapsulation and protection of hydrophobic bioactives: A review. Front. Nutr.Nutr. **9**, 999373 (2022)
37 T. Chuacharoen, C.M. Sabliov, Development of coating material by incorporating curcumin-loaded zein nanoparticles to maintain the quality of mango (Mangifera indica L. cv. Nam Dokmai). J. Agric. Food. Res. **10**, 100444 (2022)
38. L.V. Guardiola-Ponce, A. Sudkamp, L. Yin, G.W. Padua, Characterization of Zein Extracted from Wet Distillers Grains. Trans. ASABE **63**, 1059–1069 (2020)
39 G.F.M. Bautista, M.L.P. Vidallon, K.C. Salamanez, E.B. Rodriguez, Nanodelivery system based on zein-alginate complexes enhances in vitro chemopreventive activity and bioavailability of pomelo [Citrus maxima (Burm.) Merr.] seed limonoids. J. Drug Deliv. Sci. Technol. **54**, 101296 (2019)
40. Z. Liu, X. Cao, S. Ren, J. Wang, H. Zhang, Physicochemical characterization of a zein prepared using a novel aqueous extraction technology and tensile properties of the zein film. Ind. Crops Prod. **130**, 57–62 (2019)
41. L. Mahalakshmi, M.M. Leena, J.A. Moses, C. Anandharamakrishnan, Micro- and nano-encapsulation of β-carotene in zein protein: size-dependent release and absorption behavior. Food Funct.Funct. **11**, 1647–1660 (2020)
42 C.C. Uclaray et al., Encapsulation of wild oregano, Plectranthus amboinicus (Lour.) Spreng, phenolic extract in baker's yeast for the postharvest control of anthracnose in papaya. J. Sci. Food Agric. Agric. **102**, 4657–4667 (2022)
43. E.B. Rodriguez, R.A. Almeda, M.L.P. Vidallon, C.T. Reyes, Enhanced bioactivity and efficient delivery of quercetin through nanoliposomal encapsulation using rice bran phospholipids. J. Sci. Food Agric. **99**, 1980–1989 (2019)
44. E.B. Rodriguez, M.L.P. Vidallon, D.J.R. Mendoza, C.T. Reyes, Health-promoting bioactivities of betalains from red dragon fruit (Hylocereus polyrhizus (Weber) Britton and Rose) peels as affected by carbohydrate encapsulation - Rodriguez - 2016 - Journal of the Science of Food and Agriculture - Wiley Online Library. J. Sci. Food Agric. **96**, 4679–4689 (2016)
45. A.B. Abulencia, M.L.P. Vidallon, R.A. Almeda, K.C. Salamanez, E.B. Rodriguez, Rice bran phospholipid-based nanovesicles for enhanced oral and topical delivery of capsaicinoids. J. Drug. Deliv. Sci. Technol. **60**, 102005 (2020)
46. M.L.P. Vidallon et al., Exploring the transition of polydopamine-shelled perfluorohexane emulsion droplets into microbubbles using small- and ultra-small-angle neutron scattering. Phys. Chem. Chem. Phys. **23**, 9843–9850 (2021)
47. M.L.P. Vidallon et al., Tracking the heat-triggered phase change of polydopamine-shelled, perfluorocarbon emulsion droplets into microbubbles using neutron scattering. J. Colloid. Interf. Sci. **607**, 836–847 (2022)
48. M.A.L. Villar, M.L.P. Vidallon, E.B. Rodriguez, Nanostructured lipid carrier for bioactive rice bran gamma-oryzanol. Food Biosci.Biosci. **50**, 102064 (2022)
49. 5 - Mathematical models of drug release. in Strategies to Modify the Drug Release from Pharmaceutical Systems (ed. Bruschi, M. L.) (Woodhead Publishing), pp. 63–86 (2015). https://doi.org/10.1016/B978-0-08-100092-2.00005-9
50. M. Ignacio, M.V. Chubynsky, G.W. Slater, Interpreting the Weibull fitting parameters for diffusion-controlled release data. Physica A. A. **486**, 486–496 (2017)
51. A.R. Mukurumbira et al., The antimicrobial efficacy of native Australian essential oils in liquid and vapour phase against foodborne pathogens and spoilage microorganisms. Food Control **151**, 109774 (2023)
52. R. Vilaplana, G. Hurtado, S. Valencia-Chamorro, Hot water dips elicit disease resistance against anthracnose caused by *Colletotrichum musae* in organic bananas (*Musa acuminata*). LWT **95**, 247–254 (2018)
53 R.C. Martins et al., Yield, seasonality and plant health care of banana 'BRS Conquista' covered with different coloured polyethylene bags. Semin. Ciências. Agrárias. **41**, 2977–2990 (2020)
54. T.J. Anderson, B.P. Lamsal, Development of new method for extraction of α-zein from corn gluten meal using different solvents. Cereal Chem. **88**, 356–362 (2011)
55. N.U. Khan, M. Sheteiwy, N. Lihua, M.M.U. Khan, Z. Han, An update on the maize zein-gene family in the post-genomics era. Food. Prod. Process. Nutr. **1**, 13 (2019)
56. J.W.J. de Folter, M.W.M. van Ruijven, K.P. Velikov, Oil-in-water Pickering emulsions stabilized by colloidal particles from the water-insoluble protein zein. Soft Matter **8**, 6807–6815 (2012)

57. L.-Y. Wu, Q.-B. Wen, X.-Q. Yang, M.-S. Xu, S.-W. Yin, Wettability, surface microstructure and mechanical properties of films based on phosphorus oxychloride-treated zein. J. Sci. Food Agric. **91**, 1222–1229 (2011)
58. X. Yu, S. Afreen, Q. Kong, J. Wang, Study on Self-Assembled Morphology and Structure Regulation of α-Zein in Ethanol-Water Mixtures. Langmuir **36**, 11975–11984 (2020)
59. S.G. Giteru, M.A. Ali, I. Oey, Recent progress in understanding fundamental interactions and applications of zein. Food. Hydrocoll. **120**, 106948 (2021)
60. T. Zhang, F. Liu, J. Wu, T. Ngai, Pickering emulsions stabilized by biocompatible particles: A review of preparation, bioapplication, and perspective. Particuology. **64**, 110–120 (2022)
61 F. Tivano, V. Chiono, Zein as a renewable material for the preparation of green nanoparticles for drug delivery. Front. Biomater. Sci. **2**, 1156403 (2023)
62. S. Tortorella et al., Zein as a versatile biopolymer: different shapes for different biomedical applications. RSC Adv. **11**, 39004–39026 (2021)
63. S.-R. Dong, H.-H. Xu, J.-Y. Ma, Z.-W. Gao, Enhanced molecular flexibility of α-zein in different polar solvents. J. Cereal Sci. **96**, 103097 (2020)
64. T. Zhang et al., Ethanol-soluble polysaccharide from sugar beet pulp for stabilizing zein nanoparticles and improving encapsulation of curcumin. Food Hydrocoll **124**, 107208 (2022)
65. G. Chen et al., Evaluation of the colloidal/chemical performance of core-shell nanoparticle formed by zein and gum Arabic. Colloids Surf. A **560**, 130–135 (2019)
66. J. Zhou et al., A non-thermal modification method to enhance the encapsulation efficiency, stability, and slow-release performance of zein-based delivery systems – Cold plasma. J. Food Eng. **345**, 111415 (2023)
67. U. Pithanthanakul et al., Encapsulation of fragrances in zein nanoparticles and use as fabric softener for textile application. Flavour Fragr. J.. Fragr. J. **36**, 365–373 (2021)
68. D.K. Takma, S. Bozkurt, M. Koç, F. Korel, H.Ş Nadeem, Characterization and encapsulation efficiency of zein nanoparticles loaded with chestnut fruit shell, cedar and sweetgum bark extracts. Food Hydrocoll. Health. **4**, 100151 (2023)
69. U. Rodsuwan et al., Preparation and characterization of gamma oryzanol loaded zein nanoparticles and its improved stability. Food Sci. Nutr.Nutr. **9**, 616–624 (2021)
70. I.B.C. Lima et al., Nanoparticles obtained from zein for encapsulation of mesalazine. Pharmaceutics **14**, 2830 (2022)
71. M. Panagiotopoulou, S. Papadaki, M. Krokida, Formation and characterization of zein electrosprayed nanoparticles containing bioactive compounds. S. Afr. J. Chem. Eng. **40**, 32–47 (2022)
72. L.S. Viswanadha, Y. Arcot, Y.-T. Lin, M.E.S. Akbulut, A comparative investigation of release kinetics of paclitaxel from natural protein and macromolecular nanocarriers in nanoscale drug delivery systems. JCIS. Open. **15**, 100120 (2024)
73. U.J. de Martín-Camacho, N. Rodríguez-Barajas, J.A. Sánchez-Burgos, A. Pérez-Larios, Weibull β value for the discernment of drug release mechanism of PLGA particles. Int. J. Pharm. **640**, 123017 (2023)
74. A. de Souza-Pollo, A. de Goes, Banana Pathology and Diseases. in *Handbook of Banana Production, Postharvest Science, Processing Technology, and Nutrition* 45–59 (John Wiley & Sons, Ltd) (2020). https://doi.org/10.1002/9781119528265.ch3.
75 F.J. Scariot, L. Foresti, A.P.L. Delamare, A.P.L.S. Echeverrigaray, Activity of monoterpenoids on the in vitro growth of two Colletotrichum species and the mode of action on C. acutatum. Pestic. Biochem. Physiol.. Biochem. Physiol. **170**, 104698 (2020)
76. J. Romero et al., Effect of latent and symptomatic infections by Colletotrichum godetiae on oil quality. Eur. J. Plant Pathol.Pathol. **163**, 545–556 (2022)
77 F. Garcia, W.-J. Lin, V. Mellano, G. Davidov-Pardo, Effect of biopolymer coatings made of zein nanoparticles and ε-polylysine as postharvest treatments on the shelf-life of avocados (Persea americana Mill. Cv. Hass). J. Agric. Food. Res. **7**, 100260 (2022)
78. A. Kocira et al., Polysaccharides as edible films and coatings: characteristics and influence on fruit and vegetable quality—A review. Agronomy **11**, 813 (2021)

Authors and Affiliations

Dana C. Punelas–Villanueva[1,2] · Ronaniel A. Almeda[1,3] · Mari Sherlin S. Chua[1] · Rico F. Tabor[4] · Mark Louis P. Vidallon[1,4,5,6,7] · Evelyn B. Rodriguez[1]

✉ Dana C. Punelas–Villanueva
dcpvpunelas@gmail.com

✉ Mark Louis P. Vidallon
mark.vidallon@baker.edu.au

1 Smart-Functional Biomaterials Laboratory, Institute of Chemistry, College of Arts and Sciences, University of the Philippines Los Baños, College, Los Baños, 4031 Laguna, Philippines

2 Department of Chemistry, College of Arts and Sciences, University of the Philippines Visayas, 5023 Miagao, Iloilo, Philippines

3 Institute of Agricultural and Biosystems Engineering, Agricultural, Food and Bio-Process Engineering, University of the Philippines Los Baños, 4031 Laguna, Philippines

4 School of Chemistry, Monash University, Clayton, VIC 3800, Australia

5 Molecular Imaging and Theranostics Laboratory, Baker Heart and Diabetes Institute, 75 Commercial Road, Melbourne, VIC 3004, Australia

6 Department of Cardiometabolic Health, University of Melbourne, Parkville, VIC 3010, Australia

7 Department of Cardiovascular Research, Translation and Implementation, La Trobe University, Bundoora VIC, Science Dr, Baker 3083, Australia